arXiv:physics/0304064v4 [physics.atom-ph] 16 Aug 2003

Equal energy sharing double photo ionization of the Helium atom at 20eV and 40eV above threshold

J. N. Das [a] K. Chakrabarti [b,*] S. Paul [a]

[a] *Department of Applied Mathematics, University College of Science, 92 Acharya Prafulla Chandra Road, Calcutta - 700 009, India.*

[b] *Department of Mathematics, Scottish Church College, 1 & 3 Urquhart Square, Calcutta - 700 006, India*

Abstract

In this article we present triple differential cross sections for equal energy sharing kinematics for double photoionization of the helium atom at 20 and 40eV above threshold in the framework of the hyperspherical partial wave theory. This supplements our earlier work [1] in which we were successful in showing fully, gauge independence of the results in our formalism. Also in this work we treat cases in which the Stokes parameter $S_1 < 1$ so that partial polarization of the photon source is also taken into account. Agreement in shape with the Convergent Close Coupling [14,17] calculation and the experiments appears to be excellent.

Key words: Double photo ionization, helium, hyperspherical, partial wave, cross section.
PACS: 32.80Fb

1 Introduction

Double photo ionization (DPI) of the helium is one of those fundamental atomic processes which has received wide attention from both theorists and experimentalists. Helium is one of the most abundant elements in stellar atmospheres and hence analysis of Helium spectra is of considerable importance in astrophysics. From the theoretical aspect, the absorption of a photon and subsequent ejection of both electrons from the Helium atom into the continuum,

* Corresponding Author
Email address: kkch@eth.net (K. Chakrabarti).

leads to a pure Coulomb three body problem which, at low incident energies, involve complex short range interactions and strong electron correlations that are difficult to treat theoretically and hence present a challenge to theorists.

Detailed discussion about existing theories of helium double photo ionization is presented in our earlier work [1]. It would still be worthwhile to mention the convergent close coupling (CCC) theory of Bray *et al* [2], 2SC theory of Pont and Shakeshaft [3] and the 3C theory of Maulbetsch and Briggs [4] since all of them have been very widely used to study the double photo ionization process. It would also be very appropriate to single out and mention the hyperspherical $\mathcal{R}$-matrix with semi classical outgoing waves (H$\mathcal{R}$M-SOW) theory of Malegat *et al* [5,6] for two reasons. First, the method has been quite successful in describing the total ionization cross section (TICS), single and triple differential cross sections (SDCS and TDCS). Secondly the method bears similarity to our calculation in the use of hyperspherical coordinates, though the techniques used in extracting scattering information is very different from ours. The H$\mathcal{R}$M-SOW method uses $\mathcal{R}$-matrix [7] method to obtain solution of the radial wave equation in the inner region bounded by a hypersphere at R_0 (R being the hyperradius). Beyond R_0 the solution of the radial equations are propagated semiclasically (see section IV of [6]). In contrast our method is fully quantum mechanical and free from any approximations, though perhaps it is more demanding on the computational resources.

The helium double photo ionization is similar to the electron impact ionization of atomic hydrogen. However, due to the $^1S^e$ symmetry of the initial state, the final state can be only of $^1P^o$ symmetry. This leads to considerable simplification in computations in contrast to e-H ionization, in which there are many more contributing states in the final channel. Also there are selection rules that are valid only for double photo ionization [4] (for a recent review see [8]).

As is well known, the DPI triple differential cross-section can be calculated in three gauges, namely length, velocity and acceleration gauges. In principle the TDCS must be independent of the choice of gauge. However, it has been shown by Lucy *et al* [9] that the TDCS results are notoriously gauge dependent unless one uses very accurate wave functions for both initial and final channels. In our previous work [1] we had been able to show that our results are largely gauge independent and length and velocity gauge results obtained were nearly identical. We now have the TDCS results in the acceleration gauge also, and we will make a brief comparison between the TDCS in the three gauges below before we study other cases. Also in our work [1] we obtained TDCS at 20eV incident photon energy and our results were for incident photon source linearly polarized with Stokes parameter $S_1 = 1$. Having obtained an essentially gauge independent formalism, in this work we present double photo ionization TDCS at 20eV and 40eV above the helium double ionization threshold 79eV. Also we choose situations in which the incident photon beam is partially

(linear) polarized, the degree of polarization being given by the Stokes parameter S_1 (for a definition of Stokes parameters see [8]. Our S_1 corresponds to S_{lin} given in section 3.2 of Ref. [8] in which the x and y axes are respectively along the major and minor axes of the polarization ellipse).

The double ionization TDCS is obtained from the transition matrix elements given by

$$T_{fi} = \langle \Psi_f^{(-)} | V_i | \Phi_i \rangle, \tag{1}$$

where $\Phi_i(\vec{r}_1, \vec{r}_2)$ is the helium ground state, $\vec{r}_1$ and $\vec{r}_2$ being the coordinates of the two electrons with respect to the helium nucleus (assumed to be at rest). $\Psi_f^{(-)}$ is the final channel continuum state and V_i is the interaction term given by

$$V_i = \vec{\epsilon} \cdot \vec{D}. \tag{2}$$

In (2) $\vec{D}$ is the dipole operator given by $\vec{D} = \vec{\nabla}_1 + \vec{\nabla}_2$ (velocity form), $\vec{D} = \omega_i(\vec{r}_1 + \vec{r}_2)$ (length form) or $\vec{D} = -\frac{1}{\omega_i}(\vec{\nabla}_1 + \vec{\nabla}_2)V$ (acceleration form), where

$$V = -\frac{1}{r_1} - \frac{1}{r_2} + \frac{1}{|\vec{r}_1 - \vec{r}_2|}$$

is the full three body interaction potential and $\vec{\epsilon}$ is the photon polarization vector. For an arbitrary degree of (linear) polarization of the incident photon beam characterized by the Stokes parameter S_1, the TDCS is given by (see [19] for example and references therein)

$$\frac{d^3\sigma}{d\Omega_1 d\Omega_2 dE_1} = (\sigma_x + \sigma_y) + \frac{S_1}{2}(\sigma_x - \sigma_y), \tag{3}$$

where σ_x and σ_y refer to TDCS calculated with polarization vectors along the x-axis and y-axis respectively.

A schematic diagram of the scattering geometry is shown in figure 1. The photon emerges from the bottom of the scattering plane along the z-axis. The two photo-electrons are ejected after collision in the direction θ_1 and θ_2 in the scattering plane.

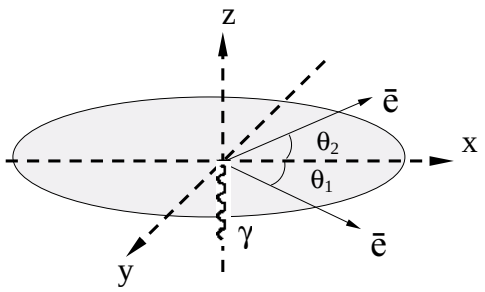

Fig. 1. Schematic diagram of the scattering geometry.

2 Theory

The hyperspherical partial wave theory is discussed in considerable detail in our earlier work [1]. Therefore we give here only the essentials.

For the Helium ground state we take a highly correlated 20 term Hylleraas type wave function given by Hart and Herzberg [10]. To calculate the final channel continuum state $\Psi_f^{(-)}$ we use hyperspherical coordinates $R = \sqrt{r_1^2 + r_2^2}$, $\alpha = \arctan(r_2/r_1)$, $\hat{r}_1 = (\theta_1, \phi_1)$, $\hat{r}_2 = (\theta_2, \phi_2)$ and $\omega = (\alpha, \hat{r}_1, \hat{r}_2)$. Also we set $P = \sqrt{p_1^2 + p_2^2}$, $\alpha_0 = \arctan(p_2/p_1)$, $\hat{p}_1 = (\theta_{p_1}, \phi_{p_1})$, $\hat{p}_2 = (\theta_{p_2}, \phi_{p_2})$ and $\omega_0 = (\alpha_0, \hat{p}_1, \hat{p}_2)$ where $\vec{r}_i$ and $\vec{p}_i$ (i = 1, 2) are the coordinates and momenta of the i^{th} particle. $\Psi_f^{(-)}$ is then expanded in hyperspherical harmonics [11,12] that are functions of the five angular variables and ℓ_1, ℓ_2, n, L, M, which are respectively the angular momenta of the two electrons, the order of the Jacobi polynomial in the hyperspherical harmonics, the total angular momentum and its projection. For a given symmetry s we decompose the final state as

$$\Psi_{fs}^{(-)}(R, \omega) = \sqrt{\frac{2}{\pi}} \sum_{\lambda} \frac{F_\lambda^s(\rho)}{\rho^{\frac{5}{2}}} \, \phi_\lambda^s(\omega) \tag{4}$$

where λ is the composite index (ℓ_1, ℓ_2, n, L, M) or $2n + \ell_1 + \ell_2$ depending on the context and $\rho = PR$ and $\phi_\lambda^s(\omega)$ are are orthogonal functions that are a product of a Jacobi polynomial $P_n^{l_1 l2}(\alpha)$ and a coupled angular momentum eigenfunction $\mathcal{Y}_{l_1 l_2}^{LM}(\Omega_1, \Omega_2)$.

F_λ^s then satisfy the infinite set of coupled differential equations

$$\Big[\frac{d^2}{d\rho^2} + 1 - \frac{\nu_\lambda \, (\nu_\lambda + 1)}{\rho^2}\Big] F_\lambda^s(\rho) + \sum_{\lambda'} \frac{2 \, \alpha_{\lambda\lambda'}^s}{P\rho} \, F_{\lambda'}^s(\rho) = 0. \tag{5}$$

Here $\alpha_{\lambda\lambda'}^s$ are the matrix elements of the full three-body interaction potential and $\nu_\lambda = \lambda + \frac{3}{2}$. Since the final channel state must have the $^1\mathrm{P}^o$ symmetry s is fixed. The contributing radial waves then correspond to $L = 1$ and (odd)

parity $\pi = -1$ so that writing $N = (\ell_1, \ell_2, n)$ and $F^s_\lambda = f_N$ the equations for the relevant set of radial waves become

$$\Big[\frac{d^2}{d\rho^2} + 1 - \frac{\nu_N\,(\nu_N+1)}{\rho^2}\Big] f_N + \sum_{N'} \frac{2\,\alpha_{NN'}}{P\rho}\, f_{N'} = 0. \tag{6}$$

For actual computations we truncate the set of equations to some maximum value N_{mx} of N. These N_{mx} equations in N_{mx} variables are solved from origin to infinity. Construction of the radial wave solution is presented in our earlier works [1,13] with considerable rigor. So we omit the details in this work. Knowing the radial wave solution, the final channel state can be found from (4) and the transition matrix elements from (1). The photoionization TDCS can then be obtained using

$$\frac{d^3\sigma}{d\Omega_1 d\Omega_2 dE_1} = \frac{2\pi^2 \alpha p_1 p_2}{\omega_i} |T_{fi}|^2. \tag{7}$$

3 Results and discussion

Convergence in our cross sections depend on two parameters, namely the number of coupled channels included in the computations and the asymptotic range parameter R_∞ where the asymptotic and the interior solutions are matched (see [1] and [13] for details). Numerical investigations show that convergence in TDCS is obtained at $R_\infty = 30000$ a.u. with 90 coupled channels. On the contrary oscillations in the SDCS persist even on increasing the asymptotic range parameter R_∞ substantially beyond 30000 a.u. This is in contrast to the H$\mathcal{R}$M-SOW method where oscillations in the SDCS die out on extending the asymptotic range. However, our computed SDCS at $E/2$ (E being the excess energy) remains more or less constant with the increase of convergence parameters. This strongly suggests that we employ a scaling technique similar to that used in the CCC theory (see [17]). Whenever the true SDCS at $E/2$ is known (from experiment or from some other theory, for example [15,16]) we normalize our computed SDCS at $E/2$ to the true SDCS by multiplying with a factor. Subsequently, we use this factor to scale our TDCS. Thus the TDCS at 20 eV incident energy have been scaled with a factor 0.8 and at 40 eV by a factor 0.6. In this way we are able to obtain absolute TDCS.

3.1 Gauge independence

As remarked earlier, in our previous work [1] we had been able to show that our work is largely gauge independent. There, independence of the TDCS results

with respect to the length and velocity gauges had been presented. We now present the TDCS results in the acceleration gauge also. These are displayed in figure 2. Except near the peaks, the length and velocity gauge results are identical. The maximal departure of the length gauge results occur near the peaks, and are respectively 20% at $\theta_1 = 0^o$, 14% at $\theta_1 = 30^o$, 14% at $\theta_1 = 60^o$ and 7% at $\theta_1 = 90^o$ from the velocity gauge. The acceleration gauge results are indistinguishable from that of the velocity gauge. The gauge independence in our results is a strong signature that our final channel wave function has the correct asymptotic and short range behaviour. Since the velocity and acceleration gauge results are identical, in subsequent calculations we compute TDCS in the acceleration gauge only, as this makes our computations much simpler for values of the Stokes parameter $S_1 < 1$.

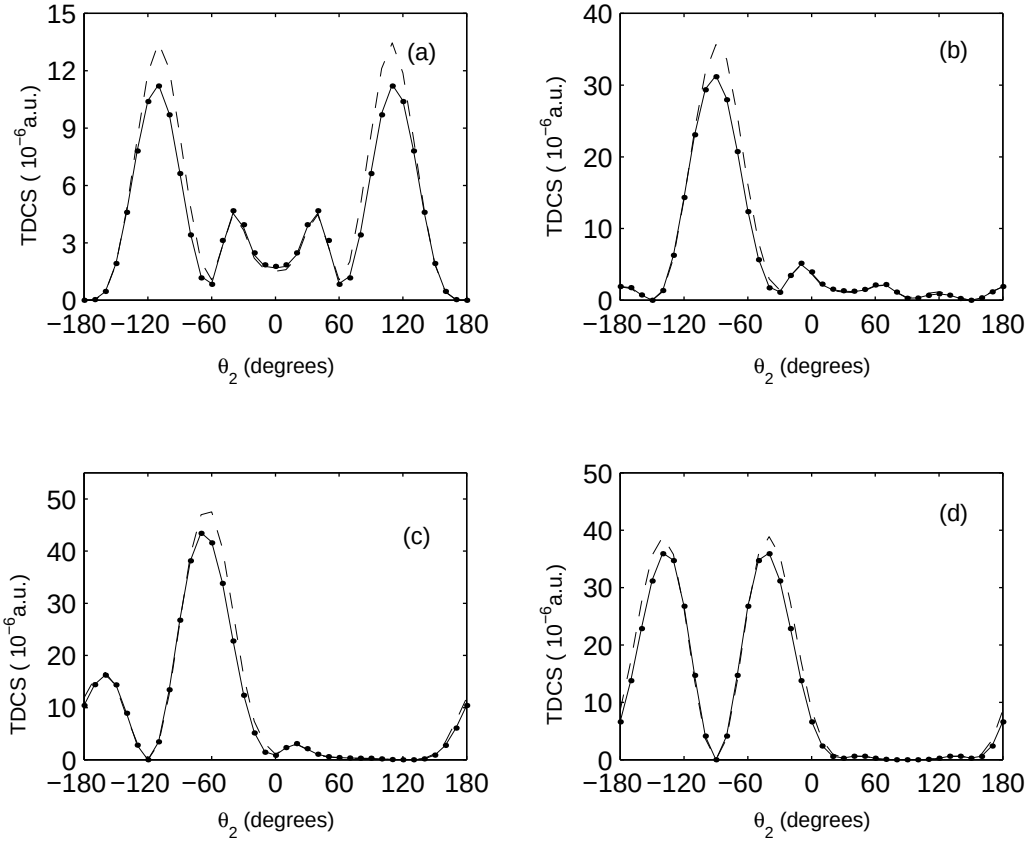

Fig. 2. TDCS for equal energy sharing double photo ionization of the helium atom at 99eV incident photon energy in units of 10^{-6} a.u. and (a) $\theta_1 = 0^o$, (b) $\theta_1 = 30^o$, (c) $\theta_1 = 60^o$, (d) $\theta_1 = 90^o$. Results are for length gauge (dashed curve), velocity gauge (continuous curve) and acceleration gauge (dotted curve). The Stokes parameter $S_1 = 1.0$.

3.2 Results for 20eV excess energy

In this section we display our results for 99eV incident photon energy and include polarization states by selecting cases with Stokes parameter $S_1 < 1$.

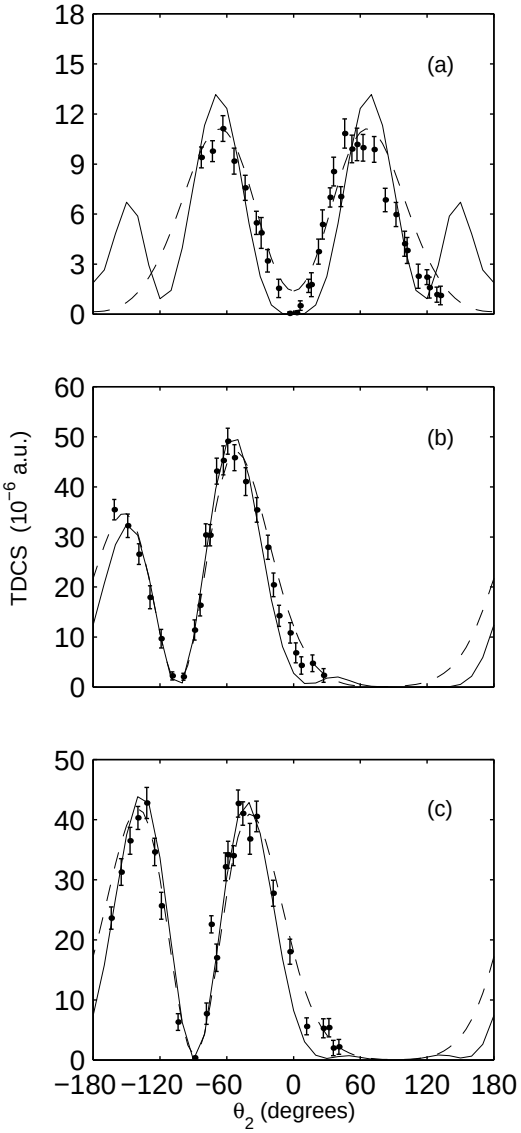

Fig. 3. TDCS for equal energy sharing double photo ionization of the helium atom at 99eV incident energy in units of 10^{-6} a.u. for (a) $\theta_1 = 180^o,\ S_1 = 0.57$, (b) $\theta_1 = -76^o,\ S_1 = 0.56$, (c) $\theta_1 = -91^o,\ S_1 = 0.53$. Theory: continuous curve - present results; dashed curve - CCC results from [14]. In (b) and (c) the CCC results have been scaled with a factor 0.52. Experiment: Filled circles with errorbars are from [8] normalized suitably with the present results in each figure.

In figure 3 we compare our results with experimental data from Briggs and Schmidt [8] and the results of the CCC theory [14,17] which are on an absolute scale. Since the experimental data are not absolute we have normalized the

data in each set to our computed results. Also the CCC results in figure 3 (b) and (c) have been scaled with a factor 0.52. The agreement of the present results with the experiment and the CCC results appears to be good everywhere in shape, except for secondary peaks near $\theta_2 = \pm 150^o$ at $\theta_1 = 180^o$ (figure 3 (a)). To see whether this additional structure in figure 3 (a) remains, we may need to perform a much larger calculation, that involves the inclusion of many more partial waves in our final state wave function.

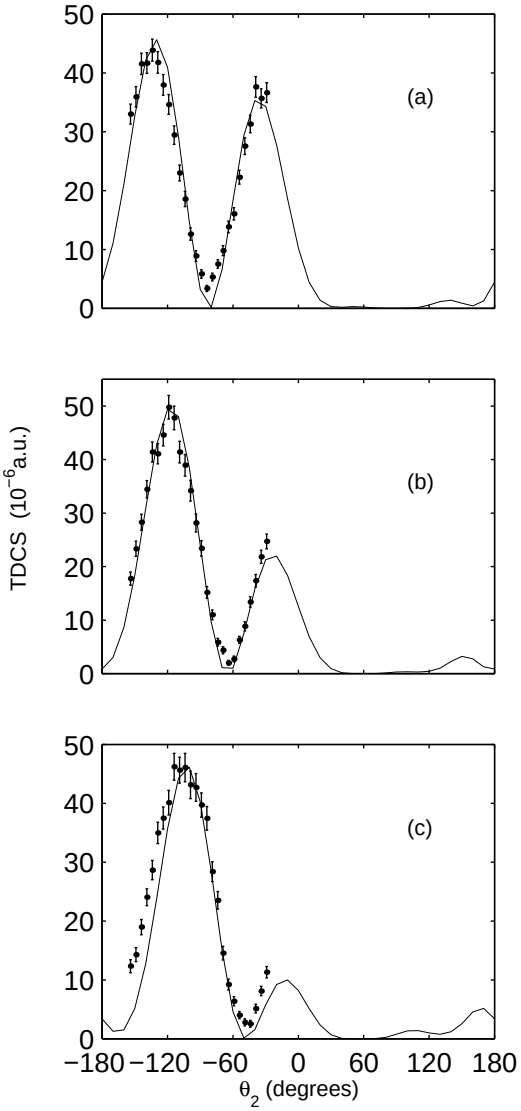

Fig. 4. TDCS for equal energy sharing double photo ionization of the helium atom at 99eV incident energy in units of 10^{-6} a.u. Theory: (a) $\theta_1 = 98^o$, (b) $\theta_1 = 115^o$, (c) $\theta_1 = 132^o$ The Stokes parameter $S_1 = 0.67$. Experiment: Filled circles with errorbars are from [18] normalized suitably with the present results by multiplying with a *single factor*.

In figure 4 we compare our results with the experimental data of Weightman *et al* [18]. The experimental data is not absolute and have been normalized to

the present results by multiplying all data with a single factor. The agreement is excellent everywhere.

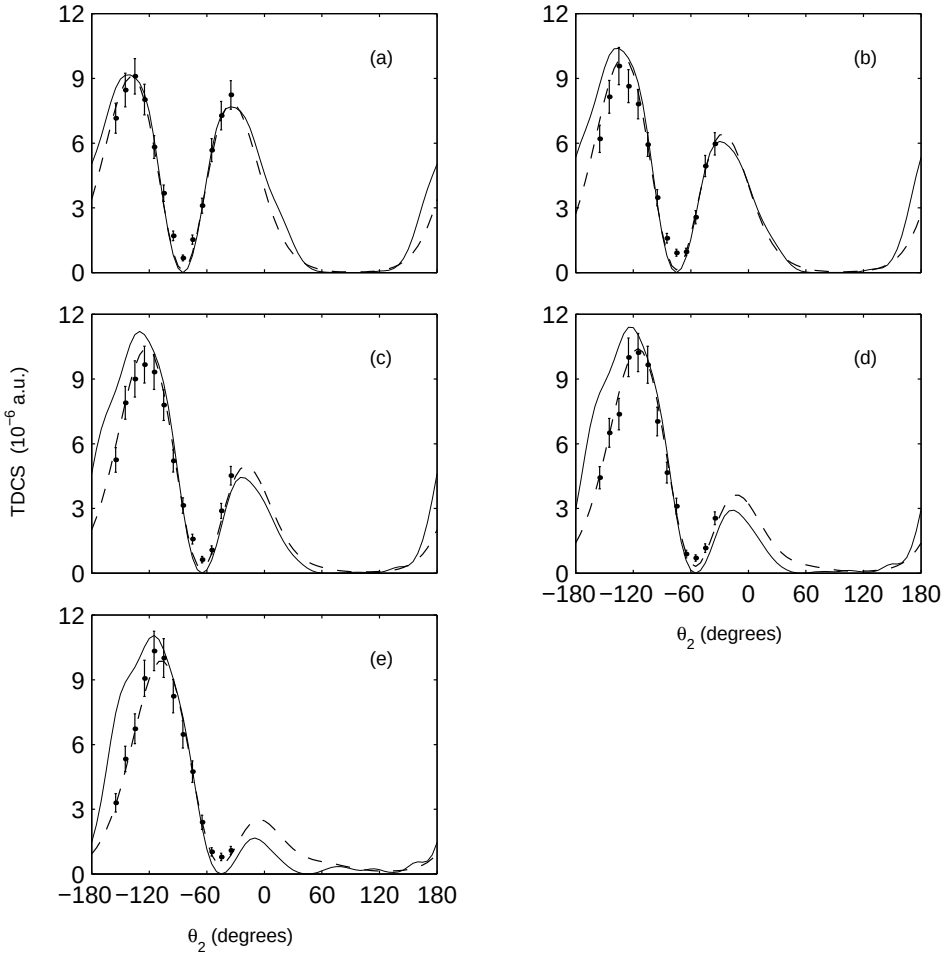

Fig. 5. TDCS for equal energy sharing double photo ionization of the helium atom at 119eV incident energy in units of 10^{-6}. Theory: (a) $\theta_1 = 95^o$, (b) $\theta_1 = 105^o$, (c) $\theta_1 = 115^o$, (d) $\theta_1 = 125^o$, (e) $\theta_1 = 135^o$. The Stokes parameter $S_1 = 0.8$. Experiment: Filled circles with errorbars are from [19] normalized suitably with the present results by multiplying with a *single factor*. The CCC results have been scaled by 0.4 for all figures.

There is the slight hint of a peak in figure 4 (a) near $\theta_2 = 180^o$ and its magnitude appears to increase in figures 4 (b) and (c). Again, confirmation of this or otherwise have to be deferred due to present limitations in our computational resources. The CCC results for this set of data are not available and hence comparisons are not made.

3.3 Results for 40eV excess energy

Figure 5 shows our results for excess energy photon energy $E = 40$ eV and Stokes parameter $S_1 = 0.8$. Shown also are the experimental results from Cvejanović *et al* [19] and the CCC results presented in Ref. [19]. The experimental points have been scaled to our theory by multiplying with 0.05 in all cases. The absolute CCC results have also been scaled by the same factor 0.4. Agreement in shape with the experimental results appear to be excellent everywhere, except in figures 5 (d) and (e) where there are slight departures around $\theta_2 = 150^0$. The CCC results are also almost identical with respect to the shapes.

4 Conclusions

In this work, we have presented results for equal energy sharing double photo ionization of the helium atom at 20 eV and 40 eV excess energy. Gauge independence of our TDCS results are shown. Cases in which the incident photon beam is partially polarized are considered. Comparisons are made with the experiments and the CCC theory wherever available and the results are seen to be consistent in shape. In the absence of absolute TDCS measurements for the chosen kinematics, it is difficult to say anything about the correctness of the magnitude of the various results. We also mention that our results presented in this work have converged approximately. For getting fully converged results, more computational facilities may be necessary. All the computations reported here were done on desktop computers with Pentium IV class CPU and 512M core memory.

In a future work, we propose to deal with unequal energy sharing kinematics. However, due to computational limitations we cannot reproduce results for extremely asymmetric energy sharing at this moment. As noted in our work [13] high Rydberg states tend to interfere with our continuum state giving undesirable results in such cases. To cope with these situations, considerably more computational resources may be necessary.

5 Acknowledgements

The authors are grateful to V. Schmidt and T. J. Reddish for providing the experimental results and to Igor Bray and Anatoli Kheifets for providing the CCC results electronically. KC acknowledges support from the University Grants Commission in the form of a Minor Research Project

F.PSW-035/02(ERO). SP is grateful to CSIR for providing a research fellowship.

References

[1] J.N. Das, K. Chakrabarti and S. Paul, J. Phys. B: At. Mol. Opt. Phys. 36(2003)2707.

[2] A. S. Kheifets and I. Bray J. Phys. B: At. Mol. Opt. Phys. 31(1998) L447

[3] M. Pont and R. Shakeshaft Phys. Rev. A51(1995)R2676.

[4] F. Maulbetsch, J. S. Briggs, J. Phys. B: At. Mol. Opt. Phys. 26 (1993)1679

[5] L. Malegat, P. Selles, A. K. Kazansky, Phys. Rev. Lett. 85(2000)4450.

[6] P. Selles, L. Malegat, A. K. Kazansky, Phys. Rev. A65(2002)032711.

[7] P. G. Burke, W. D. Robb., Adv. At. Mol. Phys. 11(1975)143.

[8] J. S. Briggs, V. Schmidt, J. Phys. B: At. Mol. Opt. Phys. 33 (2000)R1.

[9] S. P. Lucy, J. Rasch, C. T. Whelan, H. R. J. Walters, J. Phys. B: At. Mol. Opt. Phys. 31(1998)1237.

[10] J. F. Hart, G. Herzburg, Phys. Rev. 112(1957)79.

[11] J. N. Das, Pramana J. Phys. 50(1998)53.

[12] C. D. Lin, Phys. Rev. A 10(1974)1986.

[13] J. N. Das, S. Paul, K. Chakrabarti, Phys. Rev. A67(2003)042717.

[14] A. S. Kheifets (2003) private communications.

[15] M. Pont, R. Shakeshaft, J. Phys. B: At. Mol. Opt. Phys. 28(1995)L571.

[16] A. S. Kheifets, I. Bray, Phys. Rev. A 62(2000)065402.

[17] H. Bräuning, R. Dörner, C. L. Cocke, M. H. Prior, B. Krässig, A. S. Kheifets, I. Bray, A. Bräuning-Demian, K. Carnes, S. Dreuil, V. Mergel, P. Richard, J. Ulrich and H. Schmidt-Böcking, J. Phys. B: At. Mol. Opt. Phys. 31(1998)5149.

[18] J. P. Wightman, S. Cvejanović, T. J. Reddish, J. Phys. B: At. Mol. Opt. Phys. 31(1998)1753.

[19] S. Cvejanović, J. P. Wightman, T. J. Reddish, F. Maulbetsch, M. A. MacDonald, A. S. Kheifets, I. Bray, J. Phys. B: At. Mol. Opt. Phys. 33(2000)265.